

Continuous weak measurement of quantum coherent oscillations

A. N. Korotkov and D. V. Averin

Department of Physics and Astronomy, SUNY Stony Brook, Stony Brook, New York 11794-3800

(Received 22 February 2001; revised manuscript received 8 May 2001; published 5 October 2001)

We consider the problem of continuous quantum measurement of coherent oscillations between two quantum states of an individual two-state system. It is shown that the interplay between the information acquisition and the backaction dephasing of the oscillations by the detector imposes a fundamental limit, equal to four, on the signal-to-noise ratio of the measurement. The limit is universal, e.g., independent of the coupling strength between the detector and system, and results from the tendency of quantum measurement to localize the system in one of the measured eigenstates.

DOI: 10.1103/PhysRevB.64.165310

PACS number(s): 73.23.-b, 03.65.Ta

Coherent oscillations between the two states of a quantum two-state system represent one of the most basic and direct manifestations of quantum mechanics and are encountered in practically all areas of physics. The question of how to measure them directly in an individual two-state system was apparently formulated¹⁻⁴ for the first time in the context of quantum dynamics of Josephson junctions, where the oscillating variable, the magnetic flux in a superconducting loop, is macroscopic. A common feature of the measurement schemes suggested in this context is the use of conventional “projective” measurements that localize the flux in one of its eigenstates and suppress the oscillations. The time evolution of the oscillations can then only be studied if the experiment is repeated many times with the same initial conditions, and the information about oscillations is contained in the probability distribution of the measurement outcomes. This means that the oscillations are effectively studied in an ensemble of systems, not in an individual system. Another, practical, disadvantage of the projective measurements is the need to control the system dynamics externally on a time scale shorter than the oscillation period, in order to allow for preparation of the initial state of the system, free evolution of the oscillations, and subsequent measurement. Since the oscillation frequency is limited from below by several factors, including decoherence time and temperature, this requirement presents at the very least a challenging technical problem. Although this problem has been solved for oscillations of charge in a Cooper-pair box,⁵ it presents considerable obstacle to direct time-domain observation of quantum-coherent oscillations in other systems, e.g., oscillations of magnetic flux in superconducting quantum interference devices (SQUID’s), which has been observed only through the spectroscopy of energy levels.⁶

The aim of our work is to point out that the problem of measurement of quantum-coherent oscillations in an individual two-state system can be somewhat simplified if projective measurements are replaced with a weak continuous measurement, and to study the quantitative characteristics of such a measurement scheme. As is emphasized frequently in the theory of quantum measurements (see, e.g., Refs. 7–9), the “textbook” projective quantum measurement requires the dynamic interaction between the system and the detector to be sufficiently strong to establish nearly perfect correlation between their states. If the interaction is weak, this does

not happen, and the measurement provides only limited information about the system. Such a weak measurement, however, perturbs the system only slightly and can be performed continuously. Below we consider quantitatively the process of continuous weak measurement of quantum-coherent oscillations. We calculate the spectral density of the detector output and show that the trade off between the acquisition of information and dephasing due to the detector backaction on the oscillations imposes a fundamental limit, equal to four, on the signal-to-noise ratio of the measurement. In this work, we use a more conventional nonselective approach to measurement, which discusses only the quantities averaged over the detector output. All the results can be reproduced within the selective description of the measurement process.¹⁰

Although the main conclusions of our work are quite general, in what follows we prefer to use the language of a particular system: two coupled quantum dots measured with a quantum-point contact. Quantum-point contacts were used as electron detectors in Refs. 11–13 and described theoretically in Refs. 14–18,10. Coherent-electron oscillations in coupled dots were observed indirectly in the dc transport under microwave irradiation.¹⁹

The Hamiltonian of the system [see inset in Fig. 1(a)] is

$$H = -\frac{1}{2}(\varepsilon\sigma_z + \Delta\sigma_x + \sigma_z U) + \sum_{ik} \varepsilon_k a_{ik}^\dagger a_{ik}, \quad (1)$$

$$U = \sum_{ij} U_{ij} \sum_{kp} a_{ik}^\dagger a_{jp}.$$

The first two terms here describes an electron oscillating between the two discrete energy states localized in the quantum dots: ε is the energy difference between the states, $-\Delta/2$ is their tunnel coupling, and the ρ ’s denote Pauli matrices. The operators a_{ik} represent point-contact electrons in the two scattering states $i=1,2$ (incident from the two contact electrodes) with momentum k . The coupling $\sigma_z U/2$ is due to an additional scattering potential $\pm U(x)/2$ created in the point contact by the electron occupying one or the other dot. The point contact is biased with a dc voltage V , so that changes in the scattering potential lead to changes in the current I through the contact. We take eV to be much smaller than both the Fermi energy in the point contact and the inverse

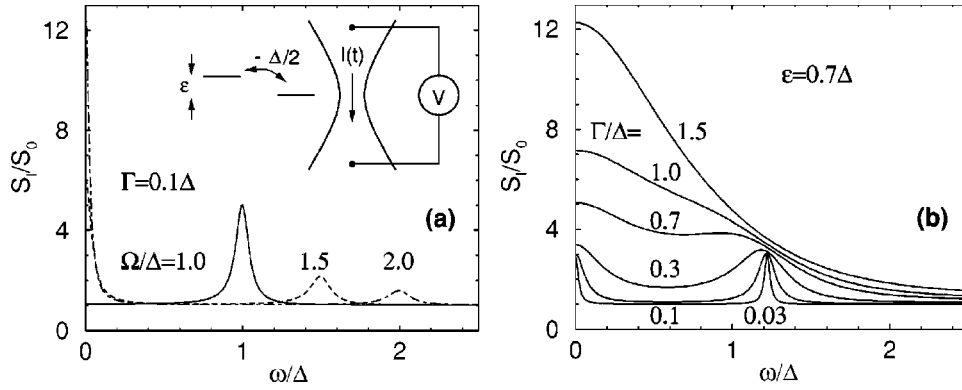


FIG. 1. The diagram [inset in (a)] of the coherent electron oscillations between the two discrete energy states in coupled quantum dots measured with a point contact. The oscillations are detected through modulation of the current $I(t)$ in the point contact biased with a voltage V . Plotted curves show the spectral density $S_I(\omega)$ of the current I in the case of symmetric coupling between the point contact and the dots for several values of (a) the energy bias ϵ between the dots reflected in the oscillation frequency $\Omega = (\Delta^2 + \epsilon^2)^{1/2}$ and (b) the rate Γ (9) of the measurement-induced dephasing.

traversal time of the contact. This allows us to linearize the energy spectrum of the point-contact electrons: $\epsilon_k = v_F k$, where v_F is the Fermi velocity, and neglect the momentum dependence of the coupling matrix elements $U_{ij} = \int dx \psi_i^*(x) U(x) \psi_j(x)$ of the perturbation U in the basis of the two scattering states $\psi_i(x)$. We also assume that the U_{ij} are sufficiently small for the point contact to operate as a linear detector, and treat the contact's response to electron in the dots in the linear-response approximation.

Quantum oscillations of electron between the dots create an oscillating component of the current I through the point contact. Since the phase of the oscillation diffuses under the backaction of the shot noise of the point contact, the oscillations are best characterized by their spectral density. To find the spectral density of the current I we choose the origin of the coordinate x along the contact in such a way that the unperturbed scattering potential is effectively symmetric, i.e., the reflection amplitudes for both scattering states are the same. Then, the current operator calculated at a point x in the asymptotic region of the scattering states is

$$I = \frac{ev_F}{L} \sum_{kp} [D(a_{1k}^\dagger a_{1p} - a_{2k}^\dagger a_{2p}) + i(DR)^{1/2} e^{-i(k-p)|x|} (a_{1k}^\dagger a_{2p} - a_{2k}^\dagger a_{1p})], \quad (2)$$

where D and $R = 1 - D$ are the transmission and reflection probabilities of the point contact, L is a normalization length, and the variation of the momentum near the Fermi points (i.e., the difference between k and p) was neglected everywhere besides the phase factor in the second term. The reason for keeping this factor will become clear later.

In the linear-response regime, the current response of the point contact is driven by the part of the perturbation U causing transitions between the two scattering states $\psi_{1,2}$. Considering the effect of this perturbation on the stationary (symmetric and antisymmetric) combinations of the scattering states, one can show that the real part of the transition matrix element U_{12} is related to the change δD of the transmission probability of the contact:

$$U_{12} = \frac{v_F}{L} \frac{\delta D + iu}{2(DR)^{1/2}}, \quad U_{21} = U_{12}^*. \quad (3)$$

The imaginary part of U_{12} , expressed through a dimensionless parameter u in Eq. (3), does not affect the current I . Qualitatively, it characterizes the degree of asymmetry in the coupling of the quantum dots to the point contact; $u = 0$ if the perturbation potential $U(x)$ is applied symmetrically with respect to the main scattering potential of the point contact.

When the point contact is used as a detector in a quantum measurement, the current I plays the role of the measurement output and should behave classically. This condition requires the spectral density of I to be much larger than the spectral density of the zero-point fluctuations in the relevant frequency range. It is satisfied when the voltage V across the point contact, which determines the magnitude and the threshold frequency of the shot noise of I , is sufficiently large, $eV \gg \epsilon, \Delta$. For the point contact to be an effective detector, eV should also be much larger than the temperature T . In this regime, it is straightforward to find the correlation functions of the perturbation U and the current I at frequencies much smaller than eV , in the zeroth order in U from Eqs. (1), (2), and (3):

$$\langle U(t)U(t+\tau) \rangle_0 = \frac{eV}{4\pi} \frac{(\delta D)^2 + u^2}{DR} \delta(\tau), \quad (4)$$

$$\langle U(t)I(t+\tau) \rangle_0 = \frac{e^2 V}{2\pi} (i\delta D + u) \delta(\tau - \eta). \quad (5)$$

The spectral density of I at low frequencies is dominated by the regular shot noise, and the current-correlation function is $K_I^{(0)}(\tau) = \langle I(t)I(t+\tau) \rangle_0 - \langle I \rangle^2 = e \langle I \rangle R \delta(\tau)$, where $\langle I \rangle = e^2 V D / \pi$. The time delay $\eta \equiv |x| / v_F$ in Eq. (4) comes from the phase factor $e^{-i(k-p)|x|}$ kept in Eq. (2), and is infinitesimally small for small traversal time of the contact. It is nevertheless important for resolving the ambiguity in averages involving the time ordering of I and U that are needed for the calculation of the current response: $i \int dt' \langle \mathcal{T} \{ I(t) U(t') \} \rangle_0$

$= e^2 V(\delta D + iu)/\pi$. Condition of the large bias voltage, together with the condition of weak dot-contact coupling, allows us to neglect renormalization of the tunnel amplitude Δ in the Hamiltonian (1) associated with this coupling—see, e.g., Ref. 20.

Expression for the current-correlation function $K_I(\tau)$ in the interaction representation with respect to U is

$$K_I(\tau) = \text{Tr}\{\tilde{\rho}(t)I(t)S^\dagger(t+\tau,t)I(t+\tau)S(t+\tau,t)\}, \quad (6)$$

where $\tilde{\rho}(t)$ is the total density matrix of the point contact and quantum dots at time t , the trace is taken over both systems, and $S(t+\tau,t) = \mathcal{T}\exp\{(-i/2)\int_t^{t+\tau} dt' \sigma_z U\}$ is the time-evolution operator. Taking the trace over the electron states in the point contact in Eq. (6) with the help of the correlation functions (4) and (5), we get

$$K_I(\tau) = K_I^{(0)}(\tau) + \frac{(\delta I)^2}{4} \langle \sigma_z \sigma_z(\tau) \rangle. \quad (7)$$

The average $\langle \dots \rangle$ in Eq. (7) is taken over the two states of the quantum dots with the stationary dot density matrix ρ established as a result of the interaction with the point contact and averaged over its dynamics. The current change $\delta I \equiv e^2(\delta D)V/\pi$ is the current response to electron oscillations between the dots, and $\sigma_z(\tau)$ now denotes the full time evolution of σ_z , driven both by the dot Hamiltonian and the interaction U with the point contact. Qualitatively, Eq. (7) shows that the current correlation function directly reflects the correlation function of the electron position in the dots given by σ_z .

The time dependence of the operator $\sigma_z(\tau)$ in Eq. (7) is obtained by tracing out the point-contact degrees of freedom in Eq. (6) with the help of the U - U correlation function (4). In this way we get the standard set of equations for the matrix elements σ_{ij} of $\sigma_z(\tau)$:

$$\dot{\sigma}_{11} = \Delta \text{Im} \sigma_{12}, \quad \dot{\sigma}_{12} = (i\varepsilon - \Gamma) \sigma_{12} - i\Delta \sigma_{11}, \quad (8)$$

and $\sigma_{22} = -\sigma_{11}$. The rate

$$\Gamma = eV \frac{(\delta D)^2 + u^2}{8\pi DR} \quad (9)$$

describes backaction dephasing of the coherent-electron oscillations between the dots by the point contact. Equation (9) shows that the dephasing rate reaches a minimum in the case of symmetric dot-contact coupling ($u=0$). In this case, the rate of dephasing by a point contact has been found in Refs. 14–16 for a single quantum-dot. In the double-dot case the situation is quite different in that the dephasing rate Γ manifests itself directly as the width of the spectral line of the quantum-coherent oscillations. Increased dephasing in the case of asymmetric dot-contact coupling was discussed qualitatively in Ref. 18 and studied experimentally in Ref. 13. Since the decrease of Γ with decreasing asymmetry u does not affect the current response of the point contact, symmetric coupling corresponds to an optimum in its operation as a detector. In this regime, the point contact represents an ideal quantum detector in a sense that the minimum value

of the dephasing rate (9) is determined purely by the rate of information acquisition about the state of the quantum dots and can be written as $\Gamma = (\delta I)^2/4S_0$, where $S_0 = 2e\langle I \rangle R$ is the spectral density of the current shot noise of the point contact.¹⁰ This part of the dephasing is fundamentally unavoidable and reflects the tendency of quantum measurement to localize the measured system in one of the eigenstates of the measured observable, in our case, the electron position σ_z .

The dot density matrix ρ satisfies the same set of equations (8), except for the normalization, $\rho_{11} + \rho_{22} = 1$, and its stationary value is $\rho = 1/2$. Solving Eqs. (8) with the initial condition $\sigma_z(0) = \sigma_z$ and averaging $\sigma_z \sigma_z(\tau)$ over $\rho = 1/2$ we find the correlation function (7) and the spectral density $S_I(\omega) = 2\int_{-\infty}^{\infty} K_I(\tau) e^{i\omega\tau} d\tau$ for $\varepsilon = 0$:

$$S_I(\omega) = S_0 + \frac{\Gamma \Omega^2 (\delta I)^2}{(\omega^2 - \Omega^2)^2 + \Gamma^2 \omega^2}. \quad (10)$$

In the case of biased dots with $\varepsilon \neq 0$, it is convenient to calculate the spectrum numerically from Eq. (8). The spectrum in this case is plotted in Fig. 1 for several values of ε and the dephasing rate Γ . For weak dephasing, $\Gamma \ll \Delta$, the spectrum consists of a zero-frequency Lorentzian that vanishes at $\varepsilon = 0$ and grows with increasing $|\varepsilon|$, and a peak at the oscillation frequency $\Omega = (\Delta^2 + \varepsilon^2)^{1/2}$. Although the width of the oscillation peak is Γ and can be small for sufficiently weak dot-contact coupling, its height cannot be arbitrarily large in comparison to the background-noise spectral density S_0 . At $\varepsilon = 0$, when the amplitude of the oscillations is maximum, the peak height is $S_{max} = (\delta I)^2/\Gamma$. Even in this case, the ratio of the peak height to the background is limited:

$$\frac{S_{max}}{S_0} = \frac{4(\delta D)^2}{(\delta D)^2 + u^2} \leq 4. \quad (11)$$

This limitation is universal, e.g., independent of the coupling strength between the dots and the point contact, and reflects quantitatively the interplay between measurement of the quantum coherent oscillations and their backaction dephasing. The fact that the height of the spectral line of the oscillations can not be much larger than the noise background means that, in the time domain, the oscillations are drowned in the shot noise.

The total intensity of the oscillation line in the spectrum:

$$\int_0^\infty [S_I(\omega) - S_0] \frac{d\omega}{2\pi} = \frac{(\delta I)^2}{4} \quad (12)$$

does depend on the strength of coupling to the point contact, increasing as the coupling becomes stronger. An interesting feature of Eq. (12) is that it stresses the impossibility of a simple classical interpretation of the quantum-coherent oscillations, since the intensity of harmonic classical oscillations of the same amplitude $\delta I/2$ would be two times smaller, and no classical signal of this amplitude could produce the oscillation line with intensity (12).

When the backaction dephasing rate Γ increases, the oscillation line broadens towards the lower frequencies, and eventually turns into the growing spectral peak at zero frequency that reflects the incoherent electron jumps between the two dots. At large Γ , when the coherent oscillations are suppressed, the rate of incoherent tunneling decreases with increasing Γ . For instance, at $\Gamma \gg \Omega$, the tunneling rate is $\gamma = \Delta^2/2\Gamma$ and the spectral density of the point-contact response has the standard Lorentzian form $S_I(\omega) - S_0 = 2\gamma(\delta I)^2/(4\gamma^2 + \omega^2)$. Suppression of the tunneling rate γ with increasing dephasing rate Γ is an example of the generic ‘‘quantum zeno effect’’ in which quantum-measurement suppresses the decay rate of a metastable state. In the context of search for the macroscopic quantum coherent oscillations, the Lorentzian spectral density has been observed and used for measuring the tunneling rate of incoherent quantum flux tunneling in SQUID’s.²¹

The maximum signal-to-noise ratio S_{max}/S_0 (11) is attained if the fundamental backaction of the detector is the only dephasing mechanism of the coherent oscillations. In the case of measurement with a point contact, the fundamental measurement-induced dephasing considered above is created by the backscattering part U_{12} (1) of the dot-contact interaction that dominates at large bias voltages V . The forward scattering U_{11} , U_{22} does not affect the current I in the contact but creates a weak additional dephasing and energy-relaxation mechanism for the oscillations. We now want to discuss the effect of such a weak relaxation on the spectral density of the oscillations noticeable if the backaction dephasing is also weak, $\Gamma \ll \Delta$.

The inclusion of the additional weak relaxation does not modify the calculations that lead to Eq. (7), apart from a trivial modification that now the average σ_z is nonvanishing, and the current-correlation function should be calculated as $K_I(\tau) = K_I^{(0)}(\tau) + (\delta I/2)^2[(1/2)\langle\sigma_z\sigma_z(\tau) + \sigma_z(\tau)\sigma_z\rangle - \langle\sigma_z\rangle^2]$. For weak coupling, it is convenient to find the time evolution of $\sigma_z(\tau)$ in the basis of eigenstates of the two-state Hamiltonian $-(\varepsilon\sigma_z + \Delta\sigma_x)/2$. Solving the Heisenberg equation of motion up to the second order in the dot-contact coupling, and tracing out the contact degrees of freedom, we get a set of equations for the evolution of the matrix elements s_{ij} of $\sigma_z(\tau)$ in the eigenstates basis:

$$\dot{s}_{jj}(\tau) = \Gamma_e \left[\frac{\varepsilon}{\Omega} - \coth\left(\frac{\Omega}{2T}\right) s_{jj} \right] + (-1)^j \frac{\Gamma\Delta^2}{2\Omega^2} (s_{11} - s_{22}),$$

$$\dot{s}_{12}(\tau) = (i\varepsilon - \Gamma_0)s_{12}, \quad (13)$$

with the initial conditions $s_{11} = -s_{22} = \varepsilon/\Omega$, and $s_{12} = -\Delta/\Omega$. The characteristic energy-relaxation rate in Eq. (13) is $\Gamma_e = v\Delta^2/\Omega$, where $v \equiv (1/\pi)(U_{11}^2 + U_{22}^2)(L/v_F)^2$, and the total dephasing rate is

$$\Gamma_0 = [v(\Delta^2\Omega \coth(\Omega/2T) + 4\varepsilon^2T) + \Gamma(2\varepsilon^2 + \Delta^2)]/2\Omega^2.$$

The dot density matrix r in the eigenstates basis satisfies similar equations, and the stationary values of its matrix elements are $r_{11} = (\Gamma_e + \Gamma_t)/2\Gamma_t$ and $r_{12} = 0$, where $\Gamma_t \equiv \Gamma_e \coth(\Omega/2T) + \Gamma\Delta^2/\Omega^2$. From these relations and Eqs. (13) we find the spectral density:

$$S_I(\omega) = S_0 + \frac{(\delta I)^2}{\Omega^2} \left\{ \varepsilon^2 \left[1 - \left(\frac{\Gamma_e}{\Gamma_t} \right)^2 \right] \frac{\Gamma_t}{\omega^2 + \Gamma_t^2} + \frac{\Delta^2}{2} \sum_{\pm} \frac{\Gamma_0}{(\omega \pm \Omega)^2 + \Gamma_0^2} \right\}. \quad (14)$$

As before, the spectral density consists of a zero-frequency Lorentzian and peaks at $\pm\Omega$ of width Γ_0 that represent the coherent electron oscillations. Energy relaxation with characteristic rate Γ_e broadens the oscillation peak and reduces its height S_{max} , so that the relative magnitude of the peak, S_{max}/S_0 decreases in comparison with its value without relaxation.

In summary, we have considered a continuous weak quantum measurement by a point contact of quantum-coherent oscillations in a two-state system, and calculated the spectral density of the output signal of the measurement. It has been shown that the backaction dephasing introduced into the oscillation dynamics by the measurement imposes the fundamental limit on its signal-to-noise ratio. We also calculated the effect of energy relaxation on the output spectrum.

The authors are grateful to K.K. Likharev and A. Maassen van den Brink for critical reading of the manuscript. This work was supported in part by ARO Grant No. DAAD199910341 and AFOSR Grant No. F496209810025.

¹A. J. Leggett and A. Garg, Phys. Rev. Lett. **54**, 857 (1985).

²L. E. Ballentine, Phys. Rev. Lett. **59**, 1493 (1987).

³A. Peres, Phys. Rev. Lett. **61**, 2019 (1988).

⁴C. D. Tesche, Phys. Rev. Lett. **64**, 2358 (1990).

⁵Y. Nakamura, Yu. A. Pashkin, and J. S. Tsai, Nature (London) **398**, 786 (1999).

⁶J. R. Friedman, V. Patel, W. Chen, S. K. Tolpygo, and J. E. Lukens, Nature (London) **406**, 43 (2000); C. H. van der Wal, A. C. J. ter Haar, F. K. Wilhelm, R. N. Schouten, C. J. P. M. Harmans, T. P. Orlando, S. Lloyd, and J. E. Mooij, Science **290**, 773 (2000).

⁷Y. Aharonov, D. Z. Albert, and L. Vaidman, Phys. Rev. Lett. **60**, 1351 (1988).

⁸V. B. Braginsky and F. Ya. Khalili, *Quantum Measurement* (Cambridge University Press, Cambridge, 1992).

⁹M. B. Mensky, Phys. Usp. **41**, 923 (1998).

¹⁰A. N. Korotkov, Phys. Rev. B **60**, 5737 (1999).

¹¹M. Field, C. G. Smith, M. Pepper, D. A. Ritchie, J. E. F. Frost, G. A. C. Jones, and D. G. Hasko, Phys. Rev. Lett. **70**, 1311 (1993).

¹²E. Buks, R. Schuster, M. Heiblum, D. Mahalu, and V. Umansky, Nature (London) **391**, 871 (1998).

¹³D. Sprinzak, E. Buks, M. Heiblum, and H. Shtrikman, Phys. Rev. Lett. **84**, 5820 (2000).

¹⁴S. A. Gurvitz, Phys. Rev. B **56**, 15215 (1997).

¹⁵Y. Levinson, Europhys. Lett. **39**, 299 (1997).

¹⁶I. L. Aleiner, N. S. Wingreen, and Y. Meir, Phys. Rev. Lett. **79**, 3740 (1997).

- ¹⁷G. Hackenbroich, B. Rosenow, and H. A. Weidenmüller, Phys. Rev. Lett. **81**, 5896 (1998).
- ¹⁸L. Stodolsky, Phys. Lett. B **459**, 193 (1999).
- ¹⁹T. H. Oosterkamp, T. Fujisawa, W. G. van der Wiel, K. Ishibashi, R. V. Hijman, S. Tarucha, and L. P. Kouwenhoven, Nature (London) **395**, 873 (1998).
- ²⁰U. Weiss, *Quantum Dissipative Systems*, (World Scientific, Singapore, 1999).
- ²¹S. Han, J. Lapointe, and J. E. Lukens, Phys. Rev. Lett. **66**, 810 (1991).